

Evolution of collectivity as a signal of quark gluon plasma formation in heavy ion collisions

Payal Mohanty, Jan-e Alam, and Bedangadas Mohanty

Variable Energy Cyclotron Centre, Kolkata 700064, India

(Received 6 August 2010; published 9 August 2011)

A measurement for studying the mass dependence of dilepton interferometry in relativistic heavy-ion collision experiments as a tool to characterize the quark gluon phase is proposed. In calculations involving dileptons, we show that the mass dependence of radii extracted from the virtual photon (dilepton) interferometry provide access to the development of collective flow with time. It is argued that the nonmonotonic variation of Hanbury Brown-Twiss radii with invariant mass of the lepton pairs signals the formation of quark gluon plasma in heavy ion collisions. Our proposal of experimentally measuring the ratio, $R_{\text{out}}/R_{\text{side}}$ for dileptons can be used to estimate the average lifetimes of the partonic as well as the hadronic phases.

DOI: [10.1103/PhysRevC.84.024903](https://doi.org/10.1103/PhysRevC.84.024903)

PACS number(s): 25.75.Cj, 12.38.Mh, 25.75.Ld, 25.75.Nq

I. INTRODUCTION

The primary goal of the nuclear collision experiments at ultra-relativistic energies is to create and study a state of matter called quark gluon plasma (QGP) [1]. Most of the experimental observables for QGP, however, contain contributions from both the partonic as well as hadronic phases. As a consequence the disentanglement of the signals for the partonic phase remains a challenge and has been successful to a limited extent [1]. Some of the probes, which are produced early in the interactions, such as jets [2] and heavy quarks [3], or real photons [4–6] and dileptons [7–10] are considered to be particularly useful.

The transverse momentum (p_T) distribution of photons reflects the temperature of the source as its production from a thermal system depend on the temperature (T) of the bath through the thermal phase space factors of the participants of the reaction that produces the photon. However, the thermal phase space factor may be changed by several factors (e.g., the transverse kick due to flow received by low- p_T photons from the low-temperature hadronic phase will mingle with the high- p_T photons from the partonic phase) making the task of detecting and characterizing QGP more difficult. For dileptons the situation is, however, different because in this case we have two kinematic variables—out of these two, the p_T spectra of lepton pairs is affected but the p_T -integrated invariant mass (M) spectra is unaltered by the flow. Moreover, it is expected that the large M pairs originate from the early time and the low M pairs are predominantly produced in the late time. Therefore, the M distribution can act as a chronometer of the heavy-ion collisions. This suggests that a simultaneous measurement of p_T and M spectra along with a judicious choice of p_T and M windows will be very useful to characterize the QGP and the hadronic phases. Precise measurements of lepton pairs in p - p collisions at a given collision energy is of paramount importance for detecting the thermal spectra in heavy-ion collisions at the same energy.

Experimental measurements of two-particle intensity interferometry has been established as a useful tool to characterize the space-time evolution of the heavy-ion collision [11]. For the case of dileptons, such an interferometry needs to be carried out over dilepton pairs, theoretically representing a study of the correlations between two virtual photons.

Although, the dilepton production rate is down by a factor of α compared to real photons, the analysis involving lepton pairs has been successfully used to get direct photon yields at RHIC [12]. In contrast to hadrons, two-particle intensity interferometry by using lepton pairs, like photons, have almost no interaction with the surrounding hadronic medium hence can provide information on the history of the evolution of the hot matter very efficiently. From the experimental point of view, dilepton interferometry encounters considerable difficulties compared to hadron interferometry due to small yield of the dileptons from the early hot and dense region of the matter and the associated large background primarily from the electromagnetic decay processes of hadrons at freeze-out. However, recent work demonstrates that it is still possible to carry out experimentally such interferometry studies [13]. The high statistics data already collected at RHIC by both STAR and PHENIX collaborations having dedicated detectors (time-of-flight [14] and hadron blind detectors [15]) with good acceptance for dilepton measurements, also augurs well for dilepton interferometry analysis.

In this work we present our proposal for carrying out an experimental measurement of dilepton interferometry at RHIC. We establish through a hydrodynamical model based space-time evolution for central 0–5% Au-Au collisions at $\sqrt{s_{\text{NN}}} = 200$ GeV the promise of such a dilepton interferometry analysis will hold out to understand the properties of the partonic phase.

II. DILEPTON INTERFEROMETRY IN HEAVY ION COLLISION

As interferometry of the dilepton pairs actually reflects correlations between two virtual photons, the analysis then concentrates on computing the Bose-Einstein correlation (BEC) function for two identical particles defined as,

$$C_2(\vec{k}_1, \vec{k}_2) = \frac{P_2(\vec{k}_1, \vec{k}_2)}{P_1(\vec{k}_1)P_1(\vec{k}_2)}, \quad (1)$$

where \vec{k}_i is the three-momentum of the particle i and $P_1(\vec{k}_i)$ and $P_2(\vec{k}_1, \vec{k}_2)$ represent the one- and two-particle inclusive lepton pair spectra respectively. The correlation function C_2

TABLE I. Values of the various parameters used in the relativistic hydrodynamical calculations.

Parameter	Value
T_i	290 MeV
τ_i	0.6 fm
T_c	175 MeV
T_{ch}	170 MeV
T_{fo}	120 MeV
EoS	2 + 1 Lattice QCD [21]

has been evaluated with the following source function:

$$P_1(\vec{k}) = \int d^4x \omega(x, k) \quad (2)$$

and

$$P_2(\vec{k}_1, \vec{k}_2) = P_1(\vec{k}_1)P_1(\vec{k}_2) + \int d^4x_1 d^4x_2 \omega(x_1, K)\omega(x_2, K) \times \cos(\Delta x^\mu \Delta k_\mu) \quad (3)$$

where $K = (k_1 + k_2)/2$, $\Delta k_\mu = k_{1\mu} - k_{2\mu} = q_\mu$, x and k are the four coordinates for position and momentum variables, respectively, and $\omega(x, k)$ is the source function related to the thermal emission of virtual photons per unit for volume R as follows:

$$\omega(x, k) = \int_{M_1^2}^{M_2^2} dM^2 \left[\frac{dR}{dM^2 d^2k_T dy} \right]. \quad (4)$$

The inclusion of the spin of the virtual photon will reduce the value of $C_2 - 1$ by $1/3$. The correlation functions can be evaluated for different average mass windows, $\langle M \rangle (\equiv M_{e^+e^-}) = (M_1 + M_2)/2$. The leading-order process through which lepton pairs are produced in QGP is $q\bar{q} \rightarrow l^+l^-$ [16]. For the low M dilepton production from the hadronic phase the decays of the light vector mesons ρ , ω , and ϕ have been considered including the continuum [4–8,17]. Since the continuum part of the vector meson spectral functions are included in the current work the processes such as four pions annihilation [18] are excluded to avoid double counting. For the space-time evolution of the system, a relativistic hydrodynamical model with cylindrical symmetry [19] and boost invariance along the longitudinal direction [20] has been used. The initial temperature (T_i) and proper thermalization time (τ_i) of the system is constrained by hadronic multiplicity (dN/dy) as $dN/dy \sim T_i^3 \tau_i$. The equation of state (EoS) that controls the rate of expansion (cooling) has been taken from the lattice QCD calculations [21]. The chemical (T_{ch}) and kinetic freeze-out (T_{fo}) temperatures are fixed by the particle ratios and the slope of the p_T spectra of hadron [22]. The values of these parameters are displayed in Table I.

With all these ingredients we evaluate the correlation function C_2 for different invariant mass windows as a function of q_{side} and q_{out} , which are related to the transverse momentum of individual pairs as follows: $q_{\text{out}} = (k_{1T}^2 - k_{2T}^2)/f(k_{1T}, k_{2T})$ and $q_{\text{side}} = 2k_{1T}k_{2T}\sqrt{1 - \cos^2(\psi_1 - \psi_2)}/f(k_{1T}, k_{2T})$, where $f(k_{1T}, k_{2T}) = \sqrt{k_{1T}^2 + k_{2T}^2 + 2k_{1T}k_{2T} \cos(\psi_1 - \psi_2)}$, $k_i =$

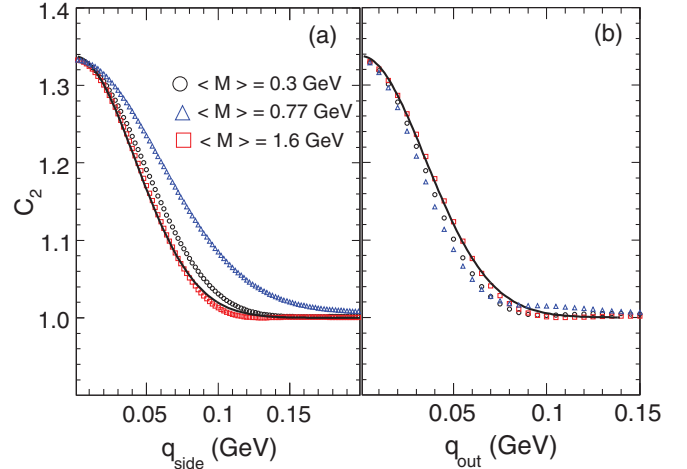


FIG. 1. (Color online) Correlation function for dilepton pairs as a function of (a) q_{side} for $k_{1T} = k_{2T} = 2$ GeV and $\psi_2 = 0$ and (b) q_{out} for $\psi_1 = \psi_2 = 0$ and $k_{1T} = 2$ GeV for three values of $\langle M \rangle$. The solid lines show the parameterization of C_2 using Eq. (5).

($M_{iT} \cosh y_i, k_{iT} \cos \psi_i, k_{iT} \sin \psi_i, M_{iT} \sinh y_i$), and $M_{iT} = \sqrt{k_{iT}^2 + \langle M \rangle^2}$.

III. RESULTS AND DISCUSSIONS

Figure 1 shows the BEC function of dilepton pairs for different values of $\langle M \rangle$ as a function of q_{side} and q_{out} . We have evaluated the C_2 for $\langle M \rangle = 0.3, 0.5, 0.77, 1.2, 1.6, 2.5$ GeV, however, in Fig. 1 we display results for only three values of $\langle M \rangle$ corresponding to low and high mass, which are expected to be dominated by radiations (see Fig. 2) from QGP ($\langle M \rangle \sim 0.3, 1.6$ GeV) and hadronic phase ($\langle M \rangle \sim 0.77$ GeV), respectively. A clear difference is seen in C_2 for different $\langle M \rangle$ windows when plotted as a function of q_{side} . The differences are, however, small when the BEC is studied as a function of q_{out} .

The source dimensions can be obtained by parametrizing the calculated correlation function of the (timelike) virtual photon with the empirical (Gaussian) form

$$C_2 = 1 + \lambda \exp(-R_i^2 q_i^2), \quad (5)$$

where the subscript i stands for out and side and λ ($= 1/3$ here) represents the degree of chaos of the source. The deviation of λ from $1/3$ will indicate the presence of nonthermal sources. A representative fit to the correlation functions is shown in Fig. 1 (solid lines).

While the radius (R_{side}) corresponding to q_{side} is closely related to the transverse size of the system and considerably affected by the collectivity, the radius (R_{out}) corresponding to q_{out} measures both the transverse size and duration of particle emission [11,23]. The extracted R_{side} and R_{out} for different $\langle M \rangle$ are shown in Fig. 3. The R_{side} shows nonmonotonic dependence on M . The R_{side} reduces with $\langle M \rangle$, reaches its minimum value at $\langle M \rangle \sim m_\rho$, and then increases again at high $\langle M \rangle$ approaching values close to the corresponding R_{side} for the QGP phase. It can be shown that $R_{\text{side}} \sim 1/(1 + E_{\text{collective}}/E_{\text{thermal}})$. In the absence of radial flow, R_{side}

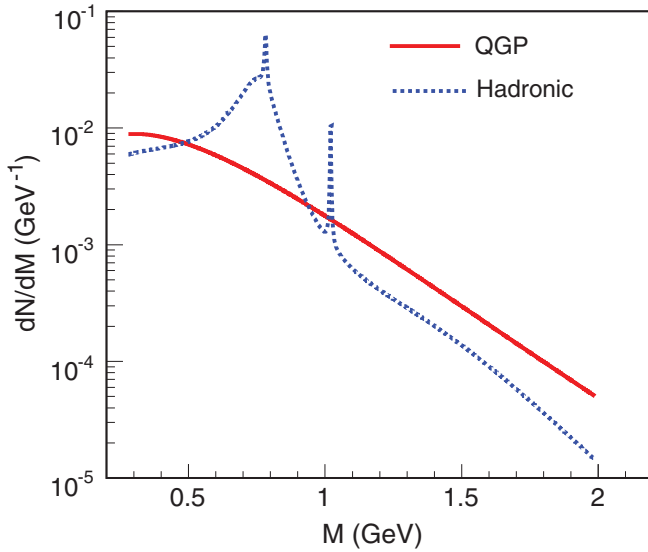


FIG. 2. (Color online) Invariant mass distribution of lepton pairs from quark matter and hadronic matter.

is independent of M . With the radial expansion of the system a rarefaction wave moves toward the center of the cylindrical geometry. As a consequence the radial size of the emission zone decreases with time. Therefore, the size of the emission zone is larger at early times and smaller at later times. The high $\langle M \rangle$ regions are dominated by the early partonic phase where the collective flow has not been developed fully (i.e., the ratio of collective to thermal energy is small hence shows larger R_{side} for the source). In contrast, the lepton pairs with $M \sim m_\rho$ are emitted from the late hadronic phase where the size of the emission zone and hence the R_{side} is smaller due to larger collective flow. The ratio of collective to thermal energy for such cases is quite large, which is reflected as a dip in the variation of R_{side} with $\langle M \rangle$ around the ρ -mass region (Fig. 3, upper panel). Thus the variation of R_{side} with M can be used as an efficient tool to measure the collectivity in various phases of the matter. The dip in R_{side} at $\langle M \rangle \sim m_\rho$ is due to the dominant contribution from the hadronic phase. The dip, in fact, vanishes if the contributions from ρ and ω are switched off (circle in Fig. 3). We observe that by keeping the ρ and ω contributions and setting radial velocity, $v_r = 0$, the dip in R_{side} vanishes, confirming the fact that the dip is caused by the radial flow of the hadronic matter. Therefore, the value of R_{side} at $\langle M \rangle \sim m_\rho$ may be used to estimate the average v_r in the hadronic phase.

The R_{out} probes both the transverse dimension and the duration of emission. Therefore, unlike R_{side} , it does not remain constant even in the absence of radial flow. The large M regions are populated by lepton pairs from the early partonic phase where the effect of flow is small and the duration of emission is also small, resulting in smaller values of R_{out} . For lepton pairs from $M \sim m_\rho$ the flow is large, which could have resulted in a dip as in R_{side} in this M region. However, R_{out} probes the duration of emission too, which is large for the hadronic phase. The larger duration compensates the reduction of R_{out} due to flow in the hadronic phase resulting in a bump in R_{out} in this region of M (Fig. 3, lower panel). Both R_{side} and R_{out}

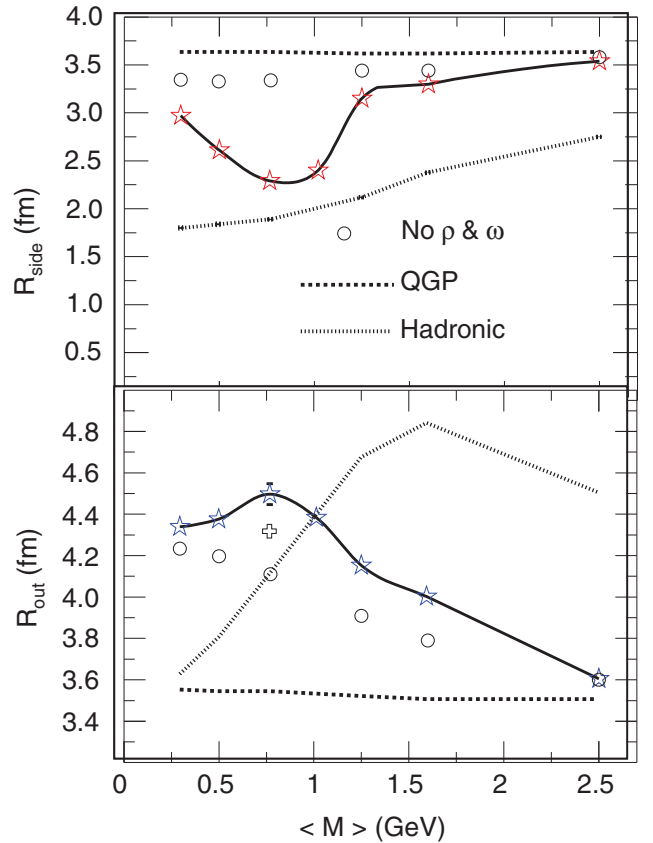


FIG. 3. (Color online) R_{side} and R_{out} as a function of $\langle M \rangle$. The dashed, dotted, and solid lines (with asterisk) indicate the HBT radii for the QGP, hadronic and total dilepton contributions from all the phases respectively. The open circles are obtained by switching off the contributions from ρ and ω .

approach QGP values for $\langle M \rangle \sim 2.5$ GeV implying dominant contributions from the partonic phase in this region of M .

It is clear from the results displayed in Fig. 2 that the high $M (> m_\phi)$ and low $M (< 0.5$ GeV) regions are dominated by the radiation from the early QGP phase when collective motion is not fully developed. As a result the sizes of the emission zones for these M regions are large. However, lepton pairs for M around ρ mass dominantly originate from the late hadronic phase when the collectivity is large and consequently the size of the homogeneous emission domain is small. This results in nonmonotonic variation of R_{side} with M as discussed above. Therefore, such a nonmonotonic behavior of the Hanbury Brown-Twiss (HBT) radii will signal the presence of two different phases during the evolution, indicating the creation of QGP, which will inevitably revert to hadrons because of the cooling due to expansion.

The quantities R_{out} and R_{side} are proportional to the average size of the system [24]. However, in the ratio $R_{\text{out}}/R_{\text{side}}$ some of the uncertainties associated with the space-time evolution get canceled out. The quantity $R_{\text{out}}/R_{\text{side}}$ gives the duration of particle emission [25–27] for various domains of M .

Figure 4 shows the variation of the ratio $R_{\text{out}}/R_{\text{side}}$ and the difference $\sqrt{R_{\text{out}}^2 - R_{\text{side}}^2}$ as a function of $\langle M \rangle$ for Au-Au collisions at $\sqrt{s_{\text{NN}}} = 200$ GeV. Both show a nonmonotonic

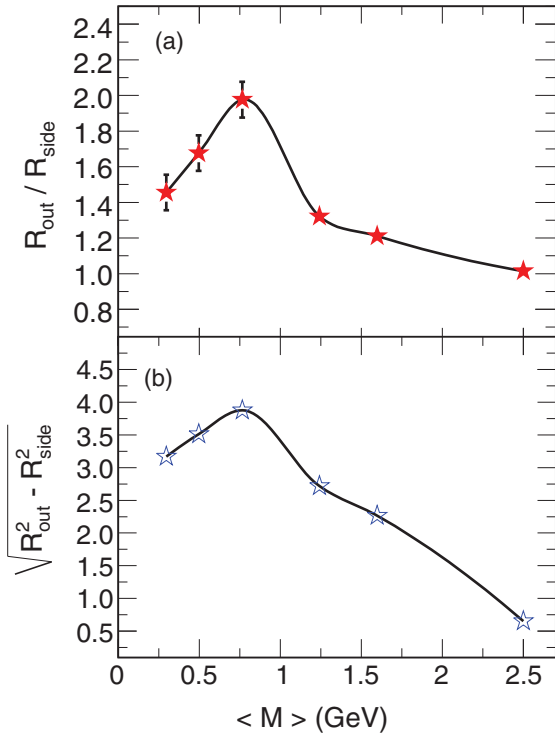


FIG. 4. (Color online) The ratio $R_{\text{out}}/R_{\text{side}}$ and the difference $\sqrt{R_{\text{out}}^2 - R_{\text{side}}^2}$ as a function of $\langle M \rangle$.

dependence on $\langle M \rangle$. The smaller values of both the quantities, particularly at high mass region, reflect the contributions from the early partonic phase of the system. The peak around ρ -meson mass reflects dominance of the contribution from the late hadronic phase as discussed before.

Now we discuss below two experimental challenges in such studies. We quote some numbers from the PHENIX measurements, keeping in mind that the situation will further improve by increasing the luminosity as well as collision energy. The number of events can be computed from the luminosity (\mathcal{L}), the p - p inelastic cross-section (σ) and the runtime (T) of the machine as,

$$N_{\text{event}} = \mathcal{L} \times \sigma \times T \quad (6)$$

For RHIC, the luminosity \mathcal{L} is of the order of $50 \times 10^{27} \text{ cm}^{-2} \text{ sec}^{-1}$ and $\sigma = 40 \text{ mb}$. If RHIC runs for 12 weeks then the number of events $N_{\text{event}} = 1.45 \times 10^{10}$. For the M , $810 \leq M \text{ (MeV)} \leq 990$, the differential number ($dN/2\pi p_T dp_T dy$) measured by the PHENIX collaboration in Au-Au collisions [10] at $\sqrt{s_{\text{NN}}}=200 \text{ GeV}$ is given by

$$\left. \frac{dN}{2\pi p_T dp_T dy} \right|_{y=0} = \frac{N_{\text{part}}}{2} \times 1.29 \times 10^{-7} \quad (7)$$

in the p_T bin 1–1.8 GeV. Therefore, the (differential) number of pairs in the above range of p_T and M is $\sim 1.45 \times 10^{10} \times \frac{N_{\text{part}}}{2} \times 1.29 \times 10^{-7} \sim \frac{N_{\text{part}}}{2} \times 1870$.

Similarly for M , $500 \leq M \text{ (MeV)} \leq 750$, the measured value of the above quantity is

$$\left. \frac{dN}{2\pi p_T dp_T dy} \right|_{y=0} = \frac{N_{\text{part}}}{2} \times 2.235 \times 10^{-7} \quad (8)$$

for the p_T bin 1.4–1.8 GeV. This indicates that the (differential) number of pairs in this kinematic domain is $\sim 1.45 \times 10^{10} \times \frac{N_{\text{part}}}{2} \times 2.235 \times 10^{-7} \sim \frac{N_{\text{part}}}{2} \times 3240$.

For 0–10 % centrality the number of participants for Au-Au collisions at $\sqrt{s_{\text{NN}}}=200 \text{ GeV}$ is about 330. The number of lepton pairs in the p_T range 1.4–1.5 GeV is $\sim 5.3 \times 10^5$ for the M window 0.5–0.75 GeV. For 12 weeks of runtime the number of events estimated with the current RHIC luminosity is $\sim 1.45 \times 10^{10}$. Then the number of pairs produced per event is $\sim 3 \times 10^{-5}$ in the kinematic range mentioned above. The probability to have two pairs of dileptons is $\sim 10^{-9}$. Therefore, roughly 10^9 events are required to make the HBT interferometry with lepton pairs possible.

It is expected that further increase in luminosity at RHIC by a factor 2 beyond the year 2012 to about $10^{29} \text{ cm}^{-2} \text{ s}^{-1}$ may be a motivating factor for such measurements. The increase in lepton pair production at higher collision energy at the large hadron collider (LHC) may also provide a reason to pursue such measurements.

The possibility of dilution of signal due to the addition of random pairs, which one may encounter in the analysis of experimental data is discussed below. We have added some mixture to the dilepton source with exponential energy distribution [i.e., we have replaced ω by $\omega + \delta\omega$ where $\delta\omega$ has exponential energy (of the pair) dependence and the weight factor is as large as that of ω itself]. Then we find that the resulting change in the HBT radii is negligibly small. This can be understood from the expression for C_2 Eq. (1)

$$C_2 = 1 + \frac{\int d^4x_1 \omega(x_1, K) \cos(\alpha_1) \int d^4x_2 \omega(x_2, K) \cos(\alpha_2)}{\int d^4x \omega(x, \vec{k}_1) \int d^4x \omega(x, \vec{k}_2)} + \frac{\int d^4x_1 \omega(x_1, K) \sin(\alpha_1) \int d^4x_2 \omega(x_2, K) \sin(\alpha_2)}{\int d^4x \omega(x, \vec{k}_1) \int d^4x \omega(x, \vec{k}_2)},$$

where

$$\begin{aligned} \alpha_1 &= \tau_1 M_{1T} \cosh(y_1 - \eta_1) - r_1 k_{1T} \cos(\theta_1 - \psi_1) \\ &\quad - \tau_1 M_{2T} \cosh(y_2 - \eta_1) + r_1 k_{2T} \cos(\theta_1 - \psi_2) \\ \alpha_2 &= \tau_2 M_{2T} \cosh(y_2 - \eta_2) - r_2 k_{2T} \cos(\theta_2 - \psi_2) \\ &\quad - \tau_2 M_{1T} \cosh(y_1 - \eta_2) + r_2 k_{1T} \cos(\theta_2 - \psi_1) \end{aligned}$$

where $x_i = (\tau_i \cosh \eta_i, r_{iT} \cos \theta_i, r_{iT} \sin \theta_i, \tau_i \sinh \eta_i)$.

It is clear that the expression for C_2 contains quadratic power of the source function both in the numerator and denominator. Therefore, changes in the source function will lead to some sort of partial cancellation (complete cancellation is not possible because the source function appears in the numerator and the denominator inside the integral with different dependent variables, K or k_i).

Now at this point some comments on the change of the spectral function of light vector mesons in the medium are in order. The modification of the spectral function of light vector mesons at nonzero temperatures and densities is a field of high contemporary interest both from the experimental and theoretical (see [6,8,28] for reviews) points of view. The enhanced production of lepton pairs at the low M domain in In-In collisions at 158 A GeV beam energy measured by the NA60 collaboration [9] indicates substantial broadening of the ρ -spectral function. In the present work we artificially

modify the spectral function of the ρ by increasing its width by a factor of two and keeping the pole mass at its vacuum value and then evaluate C_2 with the modified spectral function to explicitly check the change in the magnitudes of the HBT radii. We observe that an increase in the width of ρ by a factor of two leads to the reduction of R_{side} by about 10% for invariant mass windows below ρ peak. This reduction is due to the contributions from the decays of broader ρ , which undergoes larger flow compared to the QGP phase. The nature of the variation of R_{side} with $\langle M \rangle$ remains unaltered. However, a huge broadening of ρ for which the contribution from the hadronic phase becomes overwhelmingly large compare to the QGP phase may alter the nature of the variation of R_{side} in the low M domain.

IV. SUMMARY

In summary, the dilepton pair correlation functions have been evaluated for Au-Au collisions at RHIC energy. The additional kinematic variable M for dilepton pairs make it a

more useful tool for characterizing the different phases of the matter formed in heavy-ion collisions compared to the HBT interferometry with direct photons. The HBT radii extracted from the dilepton correlation functions show nonmonotonic dependence on the invariant mass, reflecting the evolution of collective flow in the system, which can be considered as a signal for the QGP formation in heavy-ion collisions. The M dependence of the $R_{\text{out}}/R_{\text{side}}$ and $\sqrt{R_{\text{out}}^2 - R_{\text{side}}^2}$, which can be experimentally measured could be used to characterize the source properties at various stages of the evolution.

ACKNOWLEDGMENTS

We are grateful to Tetsufumi Hirano for providing us the hadronic chemical potentials. We thank Nu Xu for very useful discussions. J.A. and P.M. were supported by India's Department of Atomic Energy-Board of Research in Nuclear Sciences (DAE-BRNS) Project Sanction No. 2005/21/5-BRNS/2455.

-
- [1] I. Arsene *et al.*, *Nucl. Phys. A* **757**, 1 (2005); B. B. Back *et al.*, *ibid.* **757**, 28 (2005); J. Adams *et al.*, *ibid.* **757**, 102 (2005); K. Adcox *et al.*, *ibid.* **757**, 184 (2005).
 - [2] J. Adams *et al.*, *Phys. Rev. Lett.* **91**, 072304 (2003); **91**, 172302 (2003); S. S. Adler *et al.*, *ibid.* **91**, 072301 (2003).
 - [3] A. Adare *et al.*, *Phys. Rev. Lett.* **98**, 172301 (2007).
 - [4] L. D. McLerran and T. Toimela, *Phys. Rev. D* **31**, 545 (1985).
 - [5] J. Alam, S. Raha, and B. Sinha, *Phys. Rep.* **273**, 243 (1996).
 - [6] J. Alam, S. Sarkar, P. Roy, T. Hatsuda, and B. Sinha, *Ann. Phys. (NY)* **286**, 159 (2001).
 - [7] C. Gale and J. I. Kapusta, *Nucl. Phys. B* **357**, 65 (1991).
 - [8] R. Rapp and J. Wambach, *Adv. Nucl. Phys.* **25**, 1 (2000).
 - [9] NA60 Collaboration, R. Arnaldi *et al.*, *Phys. Rev. Lett.* **96**, 162302 (2006); **100**, 022302 (2008).
 - [10] A. Adare *et al.*, *Phys. Rev. C* **81**, 034911 (2010).
 - [11] U. Heinz and B. V. Jacak, *Ann. Rev. Nucl. Part. Sci.* **49**, 529 (1999); T. Csörgo and B. Lörstad, *Phys. Rev. C* **54**, 1390 (1996); B. R. Schlei and N. Xu, *ibid.* **54**, R2155 (1996); D. H. Rischke and M. Gyulassy, *Nucl. Phys. A* **608**, 479 (1996).
 - [12] A. Adare *et al.*, *Phys. Rev. Lett.* **104**, 132301 (2010).
 - [13] D. Peressounko, *Phys. Rev. C* **67**, 014905 (2003); J. Alam, B. Mohanty, P. Roy, S. Sarkar, and B. Sinha, *ibid.* **67**, 054902 (2003); S. A. Bass, B. Muller, and D. K. Srivastava, *Phys. Rev. Lett.* **93**, 162301 (2004).
 - [14] B. Bonner *et al.*, *Nucl. Instrum. Methods Phys. Res., Sect. A* **508**, 181 (2003).
 - [15] A. Kozlov *et al.*, *Nucl. Instrum. Methods Phys. Res., Sect. A* **523**, 345 (2004).
 - [16] J. Cleymans, J. Fingberg, and K. Redlich, *Phys. Rev. D* **35**, 2153 (1987).
 - [17] E. V. Shuryak, *Rev. Mod. Phys.* **65**, 1 (1993).
 - [18] P. Lichard and J. Juran, *Phys. Rev. D* **76**, 094030 (2007).
 - [19] H. von Gersdorff, L. McLerran, M. Kataja, and P. V. Ruuskanen, *Phys. Rev. D* **34**, 794 (1986).
 - [20] J. D. Bjorken, *Phys. Rev. D* **27**, 140 (1983).
 - [21] C. Bernard *et al.*, *Phys. Rev. D* **75**, 094505 (2007).
 - [22] T. Hirano and K. Tsuda, *Phys. Rev. C* **66**, 054905 (2002).
 - [23] U. A. Weidemann and U. Heinz, *Phys. Rep.* **319**, 145 (1999).
 - [24] D. H. Rischke and M. Gyulassy, *Nucl. Phys. A* **608**, 479 (1996).
 - [25] M. Herrmann and G. F. Bertsch, *Phys. Rev. C* **51**, 328 (1995).
 - [26] S. Chapman, P. Scotto, and U. Heinz, *Phys. Rev. Lett.* **74**, 4400 (1995).
 - [27] S. Pratt, *Phys. Rev. D* **33**, 1314 (1986).
 - [28] G. E. Brown and M. Rho, *Phys. Rep.* **269**, 333 (1996).